

Mpemba effect in terms of mean first passage time

Matthew R. Walker

Department of Physics, University of Virginia, Charlottesville, VA 22904, USA

Marija Vucelja*

*Department of Physics, University of Virginia, Charlottesville, VA 22904, USA and
Department of Mathematics, University of Virginia, Charlottesville, VA 22904, USA*

The Mpemba effect occurs when a system prepared at a hot temperature cools down faster to the bath temperature than an identical system starting at a warm temperature. We derive the condition for the Mpemba effect in the small-diffusion limit of overdamped Langevin dynamics on a double-well potential. Our results show the strong Mpemba effect occurs when the probability of being in a well at initial and bath temperature match, which agrees with experiments. We also derive the conditions for the weak Mpemba effect and express the conditions for the effects in terms of mean first passage time.

Keywords: Anomalous thermal relaxation, Mpemba effect, overdamped Langevin dynamics, Double-well potential, Kramers' escape rate, Mean first passage time

Rapid cooling or heating of a physical system can lead to unusual thermal relaxation phenomena. A prime example of anomalous thermal relaxation is the Mpemba effect. The phenomenon occurs when a system prepared at a hot temperature overtakes an identical system prepared at a warm temperature and equilibrates faster to the cold environment [1]. A related effect exists in heating [1, 2]. Comparing two identical physical systems in their relaxation to the environment, one expects that the system with a smaller mismatch between its own and the environment's temperature would thermalize faster – yet it is not always the case. The Mpemba effect has been observed: water [3, 4], clathrate hydrates [5], magnetic systems [6], polymers [7], and colloidal particle systems [8]. Numerically it has been seen in spin-glasses [9], systems without equipartition [10], driven granular gasses [11–18], cold gasses [19], quantum systems [20–22], and antiferromagnets [1, 23–26]. The copious observations imply that the effect is general. It was studied in several theoretical works [1, 23, 27–31].

The prevalence of the effect suggests that in understanding such "shortcuts" to thermalization, we might gain insight into a general aspect of nonequilibrium statistical mechanics. On the practical level, the Mpemba effect is closely tied to optimal heating and cooling protocols and efficient sampling of phase spaces. It is thus of broad interest to industry and science to characterize this effect. To study the Mpemba effect as a paradigm, we use the overdamped Langevin dynamics on a double-well potential. Our enabling example has wide applications, from chemical reactions, polymers, colloids, escapes of metastable states, models of quantum tunneling, and scalar field theories. For a classical point particle in a potential with a metastable state this problem is well studied Kramers' escape problem [32–36]. However, even in this simple setting, it is unknown when the Mpemba effect occurs.

This letter derives the necessary conditions for the Mpemba effect in the small-diffusion limit of overdamped Langevin dynamics on a double-well potential. The condition for the effect is expressed in terms of mean first passage times. Our results agree with the experiments of Kumar and Bechhoefer [8], who looked at the Mpemba effect for a thermal quench of a colloidal system in water.

The plan of the paper is as follows. First, we introduce the model and the Mpemba effect. Next, we derive the necessary conditions for the Mpemba effect. Our analytical results are in the small-diffusion and large barrier limit, where the Kramers' problem is analytically solvable.

Model – We consider an overdamped Langevin dynamics of a particle on a double-well potential U , schematically shown on Fig. 1, and in a thermal bath of solvent molecules. The particle's trajectory $x(t)$ obeys

$$\gamma \frac{d}{dt} x(t) = -\frac{1}{m} U'[x(t)] + \Gamma(t), \quad (1)$$

where $-U' \equiv -dU/dx$ is the force, γ is the friction coefficient, and $\Gamma(t)$ is the thermal noise per unit mass. At times much larger than the collision time between the particle and the solvent $\Gamma(t)$ obeys Gaussian statistics, with $\mathbb{E}[\Gamma(t)] = 0$ and $\mathbb{E}[\Gamma(t)\Gamma(t')] = 2\gamma(k_B T_b/m)\delta(t-t')$. The diffusion coefficient is $k_B T_b/m\gamma$. Below, we set the Boltzmann constant and particle mass to unity ($k_B = 1$, $m = 1$). The corresponding Fokker-Planck (FP) equation describes the evolution of a probability density, $p(x, t)$, of having a particle at time t at coordinate x ,

$$\partial_t p(x, t) = \frac{1}{\gamma} \partial_x [U'(x) + T_b \partial_x] p(x, t) \equiv \mathcal{L} p(x, t), \quad (2)$$

where \mathcal{L} is the FP operator. We also denote the probability current density, $j(x, t)$, as $\partial_t p(x, t) \equiv -\partial_x j(x, t)$. The system is closed and we thus have reflective boundary conditions. The stationary distribution is the Boltzmann

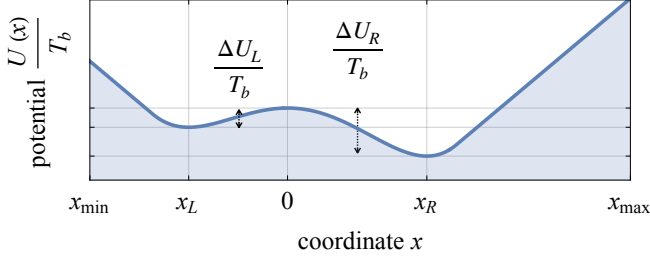


Figure 1. Double-well potential $U(x)$ with the barrier centered at $x = 0$, and minima at x_L and x_R . The barrier heights are ΔU_L and ΔU_R .

distribution,

$$\pi_{T_b}(x) = \frac{1}{Z(T_b)} e^{-\frac{U(x)}{T_b}}, \quad (3)$$

where $Z(T_b) \equiv \int_{x_{\min}}^{x_{\max}} \exp[-U(x)/T_b] dx$ is the partition function.

The scalar product is defined as $\langle u, v \rangle \equiv \int_{x_{\min}}^{x_{\max}} u(x)v(x) dx$ and the adjoint operator of the FP operator is $\mathcal{L}^\dagger = \gamma^{-1}[-U'\partial_x + T_b\partial_x^2]$. The corresponding eigenvalue problems are: $\mathcal{L}v_i = \lambda_i v_i$ and $\mathcal{L}^\dagger u_i = \lambda_i u_i$. The two eigenfunctions are related as $u_i(x) = \exp[U(x)/T_b]v_i(x)$. The eigenvalues are ordered with $\lambda_1 = 0$ being the eigenvalue corresponding to π_{T_b} and others are negative: $0 > \lambda_2 \geq \lambda_3 \geq \dots$. The probability density $p(x, t)$ is

$$p(x, t) = \pi_{T_b}(x) + \sum_{i>1} a_i e^{\lambda_i t} v_i(x), \quad (4)$$

with overlap coefficients

$$a_i \equiv \frac{\langle u_i, p_{\text{init}} \rangle}{\langle u_i, v_i \rangle}, \quad (5)$$

where p_{init} is the initial condition.

Strong and weak Mpemba effect – We assume that the system starts from equilibrium at temperature T , π_T , and consider cases with a gap between the second and the third eigenvalue, $\lambda_2 > \lambda_3$. The strong Mpemba effect happens when the overlap a_2 , defined in Eq. (5), is zero, i.e., when

$$\langle u_2 \rangle_T = 0, \quad (6)$$

where $\langle \cdot \rangle_T$ is the equilibrium expectation value at temperature T . The strong Mpemba effect is characterized by a jump of relaxation time from $-\lambda_2^{-1}$ to $-\lambda_3^{-1}$, and hence exponentially faster relaxation toward equilibrium. It occurs for initial conditions that are orthogonal to the slowest relaxation mode. The strong Mpemba effect was introduced by Klich, Raz, Hirschberg, and Vucelja in [23], and experimentally first observed by Kumar and Bechhoefer [8]. The strong Mpemba effect implies the

weak Mpemba effect, which happens when a_2 is a non-monotonic function of initial temperature T [1], i.e., when $\partial_T a_2 = 0$, which for finite T reduces to

$$\langle u_2 U \rangle_T - \langle u_2 \rangle_T \langle U \rangle_T = 0. \quad (7)$$

Next we find λ_2 and u_2 .

Spectrum of the adjoint FP operator – For the spectrum of the adjoint FP operator, we look at the following eigenvalue problem

$$\partial_x e^{-\frac{U(x)}{T_b}} \partial_x u_i(x) = \frac{\gamma \lambda_i}{T_b} e^{-\frac{U(x)}{T_b}} u_i(x). \quad (8)$$

Integrating the equation from x_{\min} to x twice and using the conservation of probability, we have

$$u_i(x) = u_i(x_{\min}) \times \left[1 + \frac{\gamma \lambda_i}{T_b} \frac{\int_{x_{\min}}^x e^{\frac{U(y)}{T_b}} dy \int_{x_{\min}}^y e^{-\frac{U(z)}{T_b}} u_i(z) dz}{u_i(x_{\min})} \right]. \quad (9)$$

For details, see the supplementary material. Similarly integrating twice from x to x_{\max} and using the boundary condition $u_i'(x_{\max}) = 0$, we get another expression for u_i ,

$$u_i(x) = u_i(x_{\max}) \alpha_i \times \left[1 + \frac{\gamma \lambda_i}{T_b} \frac{\int_x^{x_{\max}} e^{\frac{U(y)}{T_b}} dy \int_y^{x_{\max}} e^{-\frac{U(z)}{T_b}} u_i(z) dz}{u_i(x_{\max})} \right], \quad (10)$$

with $\alpha_i \equiv u_i(x_{\max})/u_i(x_{\min})$.

In the small-diffusion limit the eigenfunction u_i over $\mathcal{D}_L \equiv [x_{\min}, 0]$ is better approximated starting from Eq. (9) than Eq. (10), and over $\mathcal{D}_R \equiv [0, x_{\max}]$ it is best to use Eq. (10). By demanding u_i is continuous at $x = 0$ we get the eigenvalue

$$\frac{\gamma \lambda_i}{T_b} = (1 - \alpha_i) \left[\alpha_i \frac{\int_0^{x_{\max}} e^{\frac{U(y)}{T_b}} dy \int_y^{x_{\max}} e^{-\frac{U(z)}{T_b}} u_i(z) dz}{u_i(x_{\max})} - \frac{\int_{x_{\min}}^0 e^{\frac{U(y)}{T_b}} dy \int_{x_{\min}}^y e^{-\frac{U(z)}{T_b}} u_i(z) dz}{u_i(x_{\min})} \right]^{-1}. \quad (11)$$

Below we derive the first nonzero eigenvalue, λ_2 , and then the corresponding left eigenfunction, u_2 .

The magnitude $-\lambda_2$ signifies the switching rate between the two wells. The so-called Kramers problem is analytically solvable in the limit of small-diffusion and large barriers, c.f. [37, 38]. Both barriers, shown on Fig. 1, should be large compared to diffusion, i.e., $|\Delta U_L| \gg T_b$ and $|\Delta U_R| \gg T_b$. In this limit, the transition rate between the wells is low, i.e., λ_2 is small. We use this to get λ_2 and u_2 . In the zeroth approximation, diffusion is so small that there are no jumps between the wells, $\lambda_2^{(0)} = 0$, this implies, that u_2 , defined in Eqs. (9) and (10), is step function

$$u_2^{(0)} = \begin{cases} u_2(x_{\min}), & x \in \mathcal{D}_L \\ u_2(x_{\max}), & x \in \mathcal{D}_R \end{cases}. \quad (12)$$

In this case, the ergodicity is broken. For what follows, it is important to note that we centered the potential so it has a local maximum at $x = 0$. The coefficient $\alpha_2^{(0)}$ we get from demanding $u_2'(x)$ is continuous at $x = 0$. In the zeroth-order approximation we have $\alpha_2^{(0)} = -\int_{x_{\min}}^0 e^{-\frac{U(z)}{T_b}} dz / \int_0^{x_{\max}} e^{-\frac{U(z)}{T_b}} dz \equiv -\Pi_L(T_b)/\Pi_R(T_b)$, where we label with $\Pi_L(T_b)$ and $\Pi_R(T_b)$ the probabilities of the particle being in left and right well at temperature T_b . Plugging in $u_2^{(0)}$, Eq. (12), in the exact expression for λ_2 , Eq. (11), we get

$$\frac{\gamma\lambda_2^{(1)}}{T_b} = -\frac{Z(T_b)}{\Pi_R(T_b)\mathcal{A}_L(0) + \Pi_L(T_b)\mathcal{A}_R(0)}, \quad (13)$$

where we denoted

$$\mathcal{A}_R(x) \equiv \int_x^{x_{\max}} e^{\frac{U(y)}{T_b}} dy \int_y^{x_{\max}} e^{-\frac{U(z)}{T_b}} dz, \quad (14)$$

$$\mathcal{A}_L(x) \equiv \int_{x_{\min}}^x e^{\frac{U(y)}{T_b}} dy \int_{x_{\min}}^y e^{-\frac{U(z)}{T_b}} dz. \quad (15)$$

The eigenvector is

$$u_2^{(1)}(x) \propto \begin{cases} 1 + \frac{\gamma\lambda_2^{(1)}}{T_b}\mathcal{A}_L(x), & x \in \mathcal{D}_L \\ \alpha_2^{(1)} + \alpha_2^{(0)}\frac{\gamma\lambda_2^{(1)}}{T_b}\mathcal{A}_R(x), & x \in \mathcal{D}_R \end{cases}. \quad (16)$$

From continuity of $u_2(x)$ at $x = 0$, we have $\alpha_2^{(1)} = \alpha_2^{(0)}$.

Note that the results for λ_2 and u_2 could have been obtained by solving for the ground state and the lowest eigenfunction of the adjoint FP operator with the inverted potential $-U(x)$ and absorbing boundary conditions since there is an exact mapping between the two problems, see e.g. [37].

Below we remain with the first nonzero corrections to λ_2 . For simplicity, we drop writing the superscripts above u_2 , λ_2 , and α_2 . Before proceeding further, it is instructive to express $\mathcal{A}_L(x)$ and $\mathcal{A}_R(x)$ in terms of mean first passage times.

Mean First Passage Time – A typical Mean First Passage Time (MFPT) scenario tracks particles that leave a domain for the first time and do not return to it, see e.g. [38]. Suppose we look at the domain \mathcal{D}_R . The motion of particles is governed by the Langevin equation Eq. (1). Also, suppose our initial point $x_0 \in \mathcal{D}_R$. The first passage time is the time the particle leaves the domain. To find the MFPT, we focus on the trajectories that have not left the domain \mathcal{D}_R before time t . The distribution of such particles obeys the FP equation

$$\partial_t \tilde{p} = \tilde{\mathcal{L}}\tilde{p}, \quad (17)$$

where $\tilde{\mathcal{L}} = \mathcal{L}$, and we added the tilde symbol to signify different initial and boundary conditions from the rest of the paper. Here the initial condition is $\tilde{p}(x, 0) = \delta(x - x_0)$ for $x_0 \in \mathcal{D}_R$ and the boundary conditions are: $\tilde{j}(x_{\max}) =$

$[\tilde{p}' + U'\tilde{p}]_{x=x_{\max}} = 0$ and $\tilde{p}(0, t) = 0$. The number of points that are still in \mathcal{D}_R at time t is

$$\tilde{P}(t, x_0) = \int_{\mathcal{D}_R} \tilde{p}(x, t) dx. \quad (18)$$

The number of points that have not left before time t but have left during time integral $(t, t + dt)$ is

$$\tilde{P}(t, x_0) - \tilde{P}(t + dt, x_0) = \rho(t, x_0)dt, \quad (19)$$

where $\rho(t, x_0)$ is the distribution of first passage times. MFPT is the first moment of t of $\rho(t, x_0)$, i.e.,

$$\tau_R(x_0) = \int_0^\infty t\rho(t, x_0) dt = \int_0^\infty \tilde{P}(t, x_0) dt. \quad (20)$$

In the 1D case, τ_R can be calculated explicitly (see the supplementary material) and leads to

$$T_b\gamma^{-1}e^{\frac{U(x)}{T_b}}\partial_x e^{-\frac{U(x)}{T_b}}\partial_x \tau_R(x) = -1, \quad (21)$$

with boundary condition $\tau_R(0) = 0$, which means that any initial point on the boundary will leave immediately. Next, we assume that MFPT at $x = x_{\max}$ approaches a constant, i.e., $\tau'(x_{\max}) = 0$. Integrating Eq. (21), twice for the right domain, we get

$$\mathcal{A}_R(x) = T_b\gamma^{-1}[\tau_R(x_{\max}) - \tau_R(x)], \quad (22)$$

for $x \in \mathcal{D}_R$. The derivation for the left domain, \mathcal{D}_L , is analogous. The MFPT τ_L satisfies $T_b\gamma^{-1}e^{\frac{U(x)}{T_b}}\partial_x e^{-\frac{U(x)}{T_b}}\partial_x \tau_L(x) = -1$, with boundary conditions $\tau_L'(x_{\min}) = 0$ and $\tau_L(0) = 0$. We integrate the equation twice and for $x \in \mathcal{D}_L$ get

$$\mathcal{A}_L(x) = T_b\gamma^{-1}[\tau_L(x_{\min}) - \tau_L(x)]. \quad (23)$$

Now, using Eqs. (23) and (22) we can write the eigenvalue as

$$\lambda_2 = -\frac{Z(T_b)}{\Pi_R(T_b)\tau_L(x_{\min}) + \Pi_L(T_b)\tau_R(x_{\max})}. \quad (24)$$

In the small-diffusion limit the exponential integrals in $Z(T_b)$, $\tau_R(x_{\max})$ and $\tau_L(x_{\min})$ are readily approximated by Laplace's method. In this limit, λ_2 reduces to the sum of Kramers' rates from one well to another (see supplementary material and c.f. [37]).

Now that we have obtained the expression for u_2 (see Eq. (16)) in terms of the MFPTs, we can write down the conditions for the Mpemba effect.

Condition for the strong Mpemba effect – Plugging in the expression for u_2 , Eq. (16), in Eq. (6), we get condition for the strong Mpemba effect

$$0 = \left(\frac{\Pi_L(T)}{\Pi_L(T_b)} - \frac{\Pi_R(T)}{\Pi_R(T_b)} \right) + \frac{\gamma\lambda_2}{T_b} \left(\langle \mathcal{A}_L \rangle_{L,T} \frac{\Pi_L(T)}{\Pi_L(T_b)} - \frac{\Pi_R(T)}{\Pi_R(T_b)} \langle \mathcal{A}_R \rangle_{R,T} \right), \quad (25)$$

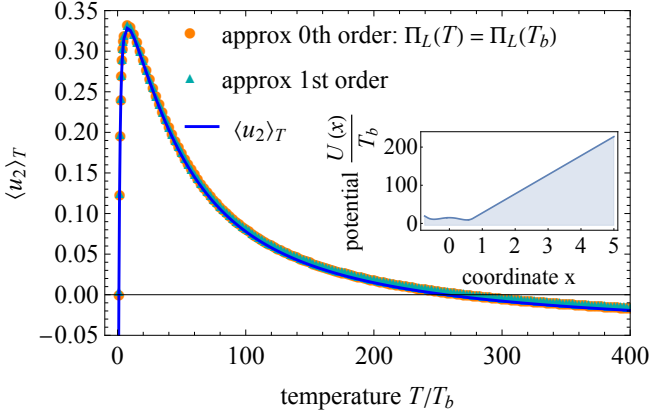


Figure 2. An example of a strong Mpemba effect at $T \approx 256 T_b$. The small-diffusion parameters are: $T_b/|\Delta U_L| = 0.24$ and $T_b/|\Delta U_R| = 0.17$. The eigenvalue is $\lambda_2 \approx -0.287$ numerically and $\lambda_2^{(1)} \approx -0.284$ with our approximation. The inset shows the potential. The condition for the strong Mpemba effect stated in Eq. (6) (blue line) and approximated with Eq. (25) (orange circles are 0th order and cyan triangles are 1st order approximation). In the zeroth order, we neglected terms proportional to $\gamma\lambda_2/T_b$ in Eq. (25). Both orders agree well with the numerics.

where $\langle \cdot \rangle_{X,T}$ is the average over \mathcal{D}_X with probability distribution $\pi(T)Z(T)/\Pi_X(T)$, where X is L or R . For vanishing small $\gamma\lambda_2/T_b$, and using $\Pi_L + \Pi_R = 1$, the above expression reduces to

$$\Pi_L(T) = \Pi_L(T_b), \quad (26)$$

which is what Kumar and Bechhoefer saw in experiment [8]. That is, they observed that the strong Mpemba effect occurs when the probability of the particle being in a well is the same for the initial and the bath temperature. Hence for vanishingly small $\gamma\lambda_2/T_b$, the strong Mpemba effect occurs when all of the equilibrium probability of being in a well is already there at the beginning. A plausible rationale is that in the limit of large barriers, it is "faster" to "drape" the probability density inside the well differently than switch between wells. Thus the strong Mpemba effect occurs when we start from close to the "right amount" of probability in each well. Corrections linear in $\gamma\lambda_2/T_b$ and λ_2 give the dependence of the condition on MFPTs. An example of the strong Mpemba effect and use of Eq. (25) is on Fig. 2.

Condition for the weak Mpemba effect – After plugging in u_2 , Eq. (16), in Eq. (7), the necessary condition for the weak Mpemba effect is

$$0 = W^{(0)} + \frac{\gamma\lambda_2}{T_b} W^{(1)}, \quad (27)$$

where

$$W^{(0)} \equiv \langle U \rangle_{L,T} \frac{\Pi_L(T)}{\Pi_L(T_b)} - \frac{\Pi_R(T)}{\Pi_R(T_b)} \langle U \rangle_{R,T} - \langle U \rangle_T \left(\frac{\Pi_L(T)}{\Pi_L(T_b)} - \frac{\Pi_R(T)}{\Pi_R(T_b)} \right), \quad (28)$$

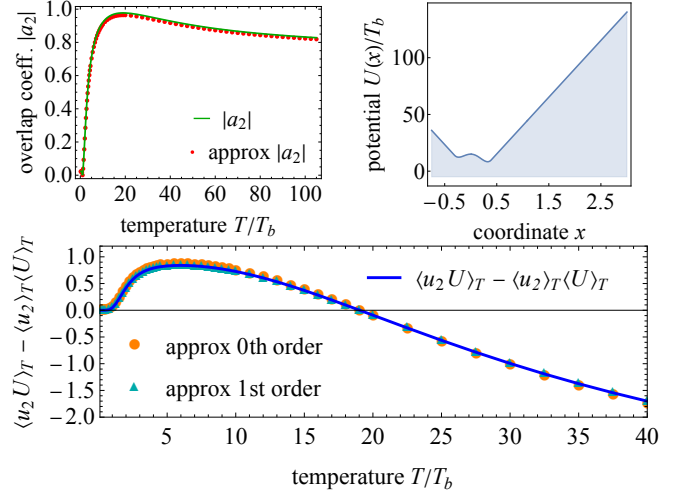


Figure 3. (top left) The overlap coefficient a_2 obtained numerically (green), and by using approximate u_2 , Eq. (16) (red circles). At initial temperature $T \approx 19 T_b$ the overlap a_2 has a local maximum, which is the hallmark of the weak Mpemba effect. (top right) The potential with small-diffusion parameters: $T_b/|\Delta U_L| = 0.36$ and $T_b/|\Delta U_R| = 0.13$. The eigenvalue is $\lambda_2 \approx -0.92$ numerically and $\lambda_2^{(1)} \approx -0.89$ with our approximation. (bottom) The condition for the weak Mpemba effect stated in Eq. (7) (blue line) and approximated with Eq. (27) (to 0th order: orange circles and 1st order: teal triangles). In the zeroth order, we neglected terms proportional to $\gamma\lambda_2/T_b$ in Eq. (27). Both orders agree well with the numerics.

and

$$W^{(1)} \equiv \langle U \mathcal{A}_L \rangle_{L,T} \frac{\Pi_L(T)}{\Pi_L(T_b)} - \frac{\Pi_R(T)}{\Pi_R(T_b)} \langle U \mathcal{A}_R \rangle_{R,T} - \langle U \rangle_T \left(\langle \mathcal{A}_L \rangle_{L,T} \frac{\Pi_L(T)}{\Pi_L(T_b)} - \frac{\Pi_R(T)}{\Pi_R(T_b)} \langle \mathcal{A}_R \rangle_{R,T} \right). \quad (29)$$

For vanishingly small $\gamma\lambda_2/T_b$ the condition for the Mpemba effect, Eq. (27), is $W^{(0)} = 0$. The dependence on MFPTs is in λ_2 and $W^{(1)}$. An example of the weak Mpemba effect and use of Eq. (27) is on Fig. 3.

The necessary conditions for the Mpemba effect, Eqs. (25) and (27), express the relation between the MFPTs, mean energy, and the pair correlation of the MFPT and energy that must hold if the effect is to occur. These equations are the main result of this letter.

No Mpemba effect for a two-level system – Notice that by reducing the problem of diffusion in a double-well potential to a two-level system with two states corresponding to the minima of the potential, we lose the Mpemba effect. In the case of a two-level system, one can see that Eqs. (25) and (27) hold only if $T = T_b$. This result is expected as for the Mpemba effect; we need at least three eigenvectors and a gap ($\lambda_2 > \lambda_3$).

Generalizations – Our results generalize to the case of spatially-dependent diffusion and predict the Mpemba effect for potentials that are a multiple of the original potential. The approximate solution for the largest nonzero

eigenvalue and eigenfunction can be generalized for multiple barriers. These generalizations are described below.

Spatially dependent diffusion – For a 1D FP equation, the coordinate dependent diffusion coefficient can always be transformed to a constant $D(T_b) > 0$, see e.g. [37]. If in the original coordinates, \tilde{x} , the diffusion coefficient was $\tilde{D}(\tilde{x}, T_b)$, then in the new coordinates, x , it is $D(T_b) = (dx/d\tilde{x})^2 \tilde{D}(\tilde{x}, T_b)$. The transformation is $x(\tilde{x}) = \int_{\tilde{x}_0}^{\tilde{x}} d\tilde{y} (D(T_b)/\tilde{D}(T_b, \tilde{y}))^{1/2}$, where choice of \tilde{x}_0 determines the value of D . The transformed potential is

$$-\frac{1}{\gamma}U'(x) = \frac{dx}{d\tilde{x}} \left(-\frac{1}{\gamma} \tilde{U}'(\tilde{x}) \right) + \left(\frac{d^2x}{d\tilde{x}^2} \right) \tilde{D}(\tilde{x}, T_b). \quad (30)$$

Due to this transform by knowing that there is a strong Mpemba effect ($a_2 = 0$) at $\{T_{\text{init}} = T, T_b\}$, force $-U'$, and diffusion coefficient $D(T_b)$, we also know that there is a strong Mpemba effect for force $-\tilde{U}'(\tilde{x})$, diffusion coefficient $\tilde{D}(\tilde{x}, T_b)$ and the same temperatures, $\{T_{\text{init}} = T, T_b\}$.

Scaling argument – Since the temperature always appears in a ratio with the potential, we have the same expression for the Boltzmann distribution and the eigenfunction u_2 for $\{U, T\}$ and for $\{\kappa U, \kappa T\}$, where κ is a constant. Thus a strong Mpemba effect for potential U , diffusion coefficient T_b/γ , and temperatures $\{T_{\text{init}} = T, T_b\}$ implies a strong Mpemba effect for potential κU , diffusion coefficient $\kappa T_b/\gamma$ and temperatures $\{T_{\text{init}} = \kappa T, \kappa T_b\}$.

Multiple barriers – Note that the approximate method for the second eigenvalue and eigenfunction for the double-well potential readily generalizes for a potential with several minima within the small-diffusion limit. Deriving the conditions for the Mpemba effect for such potentials requires separate consideration.

Discussion – We derive the necessary conditions for the Mpemba effect in the case of overdamped Langevin dynamics on a double-well potential. Our results predict the initial temperatures that lead to the Mpemba effect via integral equations that contain probabilities to be in the two wells and mean first passage times. The exponential integrals in the conditions can be readily evaluated by Laplace's method. For the strong Mpemba effect, our findings, in the leading order, agree with the experiments of Kumar and Bechhoefer [8], who observed the strong Mpemba effect when the probabilities of being in a well at the initial temperature and the bath temperature match. With large barriers, it is "faster" to rearrange the probability within the well than to switch between wells; thus, it is plausible that the initial conditions leading to the strong Mpemba effect would be the one with the "right amount" (the same amount as in equilibrium) of probability in the wells. We also derive the conditions for the weak Mpemba effect, which would be wonderful to see in an experiment.

The overdamped Langevin dynamics is a phenomenological description of many systems; thus it is interesting

to see the physical interpretation of the Mpemba effect conditions in specific cases.

This material is based upon work supported by the National Science Foundation under Grant No. DMR-1944539. MV and MRW acknowledge discussions with Gregory Falkovich, David Mukamel, Baruch Meerson, Oren Raz, Gianluca Teza, Roi Holzman, Aaron Winn, Shlomi Reuveni, Eli Barkai, and Peter Arnold. This work would not have been possible had MV not been invited to coffee at a critical moment to discuss anything and everything except the work of this paper.

* mvucelja@virginia.edu

- [1] Z. Lu and O. Raz, Proc. Natl. Acad. Sci. U.S.A. **114**, 5083 (2017).
- [2] A. Kumar, R. Chétrite, and J. Bechhoefer, Proc Natl Acad Sci U S A **119**, e2118484119 (2022).
- [3] M. Jeng, American Journal of Physics **74**, 514 (2006).
- [4] E. B. Mpemba and D. G. Osborne, Phys. Educ. **4**, 172 (1969).
- [5] Y.-H. Ahn, H. Kang, D.-Y. Koh, and H. Lee, Korean J. Chem. Eng. **33**, 1903 (2016).
- [6] P. Chaddah, S. Dash, K. Kumar, and A. Banerjee, "Overtaking while approaching equilibrium," (2010), arXiv:1011.3598 [cond-mat, physics:physics].
- [7] C. Hu, J. Li, S. Huang, H. Li, C. Luo, J. Chen, S. Jiang, and L. An, Crystal Growth & Design **18**, 5757 (2018), publisher: American Chemical Society.
- [8] A. Kumar and J. Bechhoefer, Nature **584**, 64 (2020), number: 7819 Publisher: Nature Publishing Group.
- [9] M. Baity-Jesi, E. Calore, A. Cruz, L. A. Fernandez, J. M. Gil-Narvión, A. Gordillo-Guerrero, D. Iñiguez, A. Lasanta, A. Maiorano, E. Marinari, V. Martin-Mayor, J. Moreno-Gordo, A. Muñoz Sudupe, D. Navarro, G. Parisi, S. Perez-Gaviro, F. Ricci-Tersenghi, J. J. Ruiz-Lorenzo, S. F. Schifano, B. Seoane, A. Tarancón, R. Tripiccone, and D. Yllanes, Proceedings of the National Academy of Sciences **116**, 15350 (2019), publisher: Proceedings of the National Academy of Sciences.
- [10] A. Gijón, A. Lasanta, and E. R. Hernández, Phys. Rev. E **100**, 032103 (2019), publisher: American Physical Society.
- [11] R. Gómez González and V. Garzó, Physics of Fluids **33**, 093315 (2021).
- [12] E. Mompó, M. A. López-Castaño, A. Lasanta, F. Vega Reyes, and A. Torrente, Physics of Fluids **33**, 062005 (2021).
- [13] A. Lasanta, F. Vega Reyes, A. Prados, and A. Santos, Phys. Rev. Lett. **119**, 148001 (2017), publisher: American Physical Society.
- [14] A. Megías and A. Santos, Frontiers in Physics **10** (2022).
- [15] A. Biswas, V. V. Prasad, and R. Rajesh, J Stat Phys **186**, 45 (2022).
- [16] A. Biswas, V. V. Prasad, and R. Rajesh, EPL **136**, 46001 (2022), publisher: EDP Sciences, IOP Publishing and Società Italiana di Fisica.
- [17] A. Torrente, M. A. López-Castaño, A. Lasanta, F. V. Reyes, A. Prados, and A. Santos, Phys Rev E **99**, 060901(R) (2019).

- [18] A. Biswas, V. V. Prasad, O. Raz, and R. Rajesh, Phys. Rev. E **102**, 012906 (2020), publisher: American Physical Society.
- [19] T. Keller, V. Torggler, S. B. Jäger, S. Schütz, H. Ritsch, and G. Morigi, New J. Phys. **20**, 025004 (2018), publisher: IOP Publishing.
- [20] A. Nava and M. Fabrizio, Phys. Rev. B **100**, 125102 (2019), publisher: American Physical Society.
- [21] S. Kochsiek, F. Carollo, and I. Lesanovsky, Phys. Rev. A **106**, 012207 (2022), publisher: American Physical Society.
- [22] F. Carollo, A. Lasanta, and I. Lesanovsky, Phys. Rev. Lett. **127**, 060401 (2021), publisher: American Physical Society.
- [23] I. Klich, O. Raz, O. Hirschberg, and M. Vucelja, Phys. Rev. X **9**, 021060 (2019), publisher: American Physical Society.
- [24] G. Teza, R. Yaacoby, and O. Raz, “Relaxation shortcuts through boundary coupling,” (2021), arXiv:2112.10187 [cond-mat].
- [25] G. Teza, R. Yaacoby, and O. Raz, “Far from equilibrium relaxation in the weak coupling limit,” (2022), arXiv:2203.11644 [cond-mat].
- [26] G. Teza, R. Yaacoby, and O. Raz, Phys. Rev. Lett. **130**, 207103 (2023), publisher: American Physical Society.
- [27] M. R. Walker and M. Vucelja, J. Stat. Mech. **2021**, 113105 (2021), publisher: IOP Publishing and SISSA.
- [28] D. M. Busiello, D. Gupta, and A. Maritan, New J. Phys. **23**, 103012 (2021), publisher: IOP Publishing.
- [29] J. Degünther and U. Seifert, EPL **139**, 41002 (2022), publisher: EDP Sciences, IOP Publishing and Società Italiana di Fisica.
- [30] J. Lin, K. Li, J. He, J. Ren, and J. Wang, Phys. Rev. E **105**, 014104 (2022), publisher: American Physical Society.
- [31] R. Holtzman and O. Raz, Commun Phys **5**, 1 (2022), number: 1 Publisher: Nature Publishing Group.
- [32] H. A. Kramers, Physica **7**, 284 (1940).
- [33] V. I. Mel’nikov, Physics Reports **209**, 1 (1991).
- [34] J. S. Langer, Annals of Physics **54**, 258 (1969).
- [35] F. Moss and P. V. E. McClintock, *Noise in Nonlinear Dynamical Systems* (New York: Cambridge University Press, 1988).
- [36] L. Pontryagin, A. Andronov, and A. Vitt, Zh. Eksp. Teor. Fiz. **3**, 165 (1933).
- [37] H. Risken, *The Fokker-Planck Equation: Methods of Solution and Applications*, edited by H. Haken, Springer Series in Synergetics, Vol. 18 (Springer, Berlin, Heidelberg, 1996).
- [38] R. Zwanzig, *Nonequilibrium Statistical Mechanics* (Oxford University Press, Oxford, New York, 2001).